



Synthesis Methods and Green Synthesis of Lanthanum Oxide Nanoparticles: A Review

Rofi Fadilah Madani¹, Irine Sofianty¹, Adani Ghina Puspita Sari¹, Rina Maryanti², and Asep Bayu Dani Nandiyanto^{1*}

¹Departemen Pendidikan Kimia, Fakultas Pendidikan Matematika dan Ilmu Pengetahuan Alam, Universitas Pendidikan Indonesia, JL. Dr. Setiabudi no. 229, Bandung 40154, Jawa Barat, Indonesia

²Departemen Pendidikan Khusus, Fakultas Ilmu Pendidikan. Universitas Pendidikan Indonesia, JL. Dr. Setiabudi no. 229, Bandung 40154, Jawa Barat, Indonesia

Received 18 July 2020, Revised 28 Aug 2020, Accepted 30 Aug 2020

Abstract

Various applications of lanthanum oxide nanoparticles are increasing industrially and in biotechnology. The purpose of this research is to review papers for various methods in the synthesis of La_2O_3 and to find out which method is more effective for the production of La_2O_3 nanoparticles. The method is based on a literature study from various journal sources with the keywords La_2O_3 synthesis and green synthesis. The discussion is divided into the La_2O_3 synthesis method and the source of La_2O_3 nanoparticles from plant extracts. The La_2O_3 synthesis studied were co-precipitation, hydrothermal reaction, solution combustion, thermal decomposition, reflux, sol-gel, sonochemistry, and spray pyrolysis. Potential sources of plant extracts are *Sesbania grandiflora*, *Juvenile maize*, *Datura metel*, *Nothopanax scutellarium*, *Physalis angulate*, and *Andrographis paniculata* for the green synthesis of La_2O_3 . From these results, the most effective method for synthesizing La_2O_3 is the hydrothermal method because many control parameters can be adjusted, the type of solvent is simple, and it produces homogeneous crystals. The most potential plant is *Physalis angulata* because of the abundant availability of plants in Indonesia and the compounds contained can be used for the pharmaceutical. The results of this literature review are expected to provide information on an effective method for synthesizing La_2O_3 .

Keywords: La_2O_3 nanoparticles synthesis, plant extract, green synthesis, nanotechnology

*Corresponding author.

E-mail address: nandiyanto@upi.edu

1. Introduction

Currently, research on the synthesis of lanthanum oxide nanoparticles with various eco-friendly methods and materials has been carried out. Lanthanum oxide nanoparticles are rare earth metals with distinctive properties making them good candidates for biomedical applications. Probes coated with lanthanum oxide nanoparticles are being developed as implantable sensors of various molecules such as glucose, phosphate, and uric acid [1]. In combination with other elements, lanthanum oxide (La_2O_3) is being developed as an optical sensing system for measuring variations in human body temperature [2]. Due to its paramagnetic properties, this drug is also being developed for targeted drug release by magnetic fields in the body. La_2O_3 suppresses bacteria [3], viruses [4], and fluorescent dyes [5], selectively binds to several proteins [6], suppresses calcium channels [7], and has light-emitting properties [8]. The potential for developing green chemistry in Indonesia is very large as a country with high biodiversity and can be used as a source of various natural materials [9].

There are advantages to nanoparticles based on drug production and delivery processes. Nanoparticles are quite easy to prepare which is why they are used in drugs after targeting a specific area. Their small size, nanoparticles penetrate tiny capillaries and are taken up by cells allowing for efficient drug accumulation in target areas in the body. Using nanoparticles in drug delivery provides good control on size and provides good protection of the encapsulated drug. Drug retention at the active site has a longer clearance time. Nanoparticles improve therapeutic efficiency as well as bioavailability. Reduces feeding/fasting variability which increases drug stability. Stable dosage forms of drugs that are unstable or have very low bioavailability in non-nanoparticulate dosage forms. While the carrier drug with nanoparticles has carrier biotoxicity. Nanoparticles do not show problems in large-scale production and sterilization but simply avoid the use of organic solvents [10-12].

Lanthanum is used in various fields such as piezoelectric materials, electrical materials, thermoelectric materials, luminescent materials, optical glass, laser materials, and various alloying materials. Lanthanum oxide is assumed to be a tissue modifier in various types of glass [13].

In this paper, we aim to discuss the synthesis of various La_2O_3 nanoparticles and plant sources derived from green synthesis methods. This paper consists of three parts: an introduction which contains information about La_2O_3 nanoparticles, green synthesis, and their applications. In the second part, various sources of La_2O_3 derived from plants are discussed and their characterization methods are discussed. The third part contains the results of the green synthesis of La_2O_3 nanoparticles derived from plant sources.

2. Current studies on the use of La₂O₃ nanoparticles

Several methods and plant species that can be used for the synthesis of La₂O₃ nanoparticles can be seen in [Table 1](#) and [Table 2](#). [Table 1](#) shows several methods of synthesizing La₂O₃, namely co-precipitation, hydrothermal reaction, solution combustion, thermal decomposition, reflux, sol-gel, sonochemical, and spray pyrolysis. [Table 2](#) shows some plants that can be used as a source of La₂O₃ nanoparticles, namely *Sesbania grandiflora*, *Juvenile maize*, *Datura metel*, *Nothopanax scutellarium*, *Andrographis paniculata*, and *Physalis angulata*.

3. Method

The method used is a literature study from various journal sources with the keywords La₂O₃ synthesis and green synthesis. Journal sources are taken from various years by discussing the application focus of La₂O₃ nanoparticles, methods of synthesizing La₂O₃ nanoparticles with various development potentials, and plant sources for green synthesis of La₂O₃ nanoparticles.

Table 1. Comparison of Methods Used in Synthesis La₂O₃ nanoparticle

Method	Synthesis procedur	Result	Advantages	Deficiency	Ref
Co-precipitation	It takes 0.1 M Lanthanum nitrate hexahydrate dissolved in distilled water with constant stirring for 30 minutes at room temperature. 0.3M dilute NaOH solution was added to the lanthanum nitrate solution dropwise with constant stirring and the solution was allowed to stand. The unreacted nitrate in the resulting precursor solution was completely removed by washing with water and ethanol several times. After the washing process is complete, the final form of the precursor solution changes color from black to whitish. Filtered to produce the final product	Based on the structural analysis, La ₂ O ₃ nanoparticles have a hexagonal structure with a slight mixture of lanthanum hydroxide and carbonate confirmed from the XRF pattern and the particle crystal sizes were found to be 41 nm (Scherrer method) and 47 nm (W-H plot results). The results of morphological analysis, the estimated average particle size is 37	- The synthesis process of La ₂ O ₃ nanoparticles uses room temperature, does not require high temperatures - The results indicate that the La ₂ O ₃ nanoparticles have a good optical response due to the high energy indirect bandgap of 5.35 eV obtained from the KM	It must get the sediment as pure as possible	[14]

Table 1. Comparison of Methods Used in Synthesis La₂O₃ nanoparticle (continued)

Method	Synthesis procedure	Result	Advantages	Deficiency	Ref
	and dried at room temperature for 96 hours. The obtained powder samples were ground using a mortar and pestle to obtain very fine La ₂ O ₃ nanoparticles.	nm with ImageJ software.	plot using the DRS reflection spectrum.		
Hydrothermal reaction	Synthesis of the La ₂ O ₃ nanorod using 0.2730 g of hexacle cyler methylammonium bromide (CTAB) was first introduced into 30 mL of distilled water under magnetic stirring at room temperature. After that, 0.5860 g Lanthanum chloride (LaCl ₃ .6H ₂ O) was added with stirring to form a homogeneous transparent solution, and 0.1–0.6 mL 25% ammonia was added dropwise to the solution to adjust the pH value of the solution from the range of 6.0–10.0. Along with the addition of ammonia, the solution turns into a colorless colloid. After vigorous stirring for 2 h, the system was transferred to a Teflon-coated stainless steel autoclave, sealed, and maintained at 80°C for 24 h. The resulting white solid product was centrifuged, washed with distilled water and ethanol to remove the remaining ions in the final product. In the end, the product is dried at 60°C	- The TEM depiction of the samples obtained at different reaction times (8 h and 12 h) showed that the nanorod length grew longer with increasing reaction time. -There is a longer La ₂ O ₃ nanorod growth with increasing reaction temperature- Changes in surfactant micelle structure with increasing pH value - The effect of increasing the number of CTAB on the morphology, the length of the La ₂ O ₃ nanorod will decrease, but the diameter of the nanorod almost does not change about (5 nm).	- The porosity of the material provides several potential applications as advanced materials with good BJH analysis showing that the porous La ₂ O ₃ has an average pore diameter of 7.9 nm.	This process is somewhat difficult for industrial production	[15]

Table 1. Comparison of Methods Used in Synthesis La₂O₃ nanoparticle (continued)

Method	Synthesis procedure	Result	Advantages	Deficiency	Ref
Solution combustion	Synthesis was carried out by mixing lanthanum nitrate with acetamide as fuel. The two reactants were mixed well and the solution was put into a muffle furnace at 600°C for 4 - 5 hours. After that, there will be solid particles. Cool to room temperature and perform some analysis on the sample. All reagents used were mixed using double distillation of water.	The structure of La ₂ O ₃ nanoparticles was obtained in a pure cubic phase. The average crystal size of the samples synthesized by this method was 42 nm. The mass percentage composition of these elements is 35.15% oxygen and 64.42% lanthanum.	- Based on FTIR analysis showed the good formation of La ₂ O ₃ nanoparticles for La-O band at 653 cm ⁻¹ and TGA/DSC stated effective material weight reduction at 350°C - Structural properties obtained by SEM reveal good porosity and porosity in the nanocrystalline La ₂ O ₃ network	- Based on the TEM analysis it has been found that the sample particles do not well in crystals due to severe agglomeration. - Method using high temperature	[16]
Thermal decomposition.	The synthesis of La ₂ O ₃ was analyzed using a scanning electron microscope (SEM model KYKY-EM 3200, China). Lanthanum oxide nanoparticles were prepared by calcining carbonate precursors. La ₂ (CO ₃) ₃ nanoparticles obtained in the initial stage were used for calcination. The precursors were thermally decomposed at 650°C in a static air	- The average particle size is in the range of 35 and 30 nm - For pure AP, 0.5% La ₂ O ₃ +AP, 2% La ₂ O ₃ +AP and 5% La ₂ O ₃ +AP determined at 728, 944, 1164 and 1590 J/g.	The results of the analysis showed a strong catalytic effect of the nanoparticles with a substantial decrease in the AP deposition temperature	The method uses very high temperature	[17]

Table 1. Comparison of Methods Used in Synthesis La₂O₃ nanoparticle (continued)

Method	Synthesis procedure	Result	Advantages	Deficiency	Ref
	the atmosphere for 3 hours. Approximately 2 grams of carbonate precursors are filled in an alumina crucible (with dimensions of 60 mm in diameter and 20 mm in height). A thin perforated copper foil was used on the head of the crucible to avoid powder dispersion in the furnace during the thermal decomposition of the precursor.		and an augmentation of the decomposition heat for the AP.		
Reflux	All materials were obtained from commercial suppliers and used without further purification. Lanthanum oxide (La ₂ O ₃) was synthesized by a simple reflux method using Lanthanum nitrate (LaN ₃ O ₉ .6H ₂ O) and Urea (NH ₂ CONH ₂) as starting and strong materials. The effect of precursor concentration on the properties of Lanthanum oxide (La ₂ O ₃) nanoparticles has been explored and reported. In a typical synthesis, it takes moles of Lanthanum nitrate and 0.01 moles of Urea dissolved in 500 ml of double-distilled water. The precursor solution was transferred into a round bottom flask and maintained at a constant temperature of 120°C for 24 h. Samples were	The XRD pattern corresponds to the samples prepared with the precursor concentrations of 0.01 and 0.1 mol, respectively. The peaks in the XRD pattern matched the JCPDS#50-0602 card, indicating the formation of La ₂ O ₃ with a monoclinic structure with lattice parameters a=10.12, b=11.94, and c=12.78. It is clear that as the precursor concentration increases, the number of peaks and peak intensity increase. The increase in peak intensity with	The reflux method seems very promising to obtain these nanoparticles at low temperature and low cost. New physical properties and new technologies in both sample preparation and device fabrication are emerging due to the development of nanoscience.	It requires a large amount of solvent	[18]

Table 1. Comparison of Methods Used in Synthesis La₂O₃ nanoparticle (continued)

Method	Synthesis procedure	Result	Advantages	Deficiency	Ref
	prepared with different concentrations of precursor (lanthanum nitrate) 0.01 and 0.1 moles. Finally, the prepared nanoparticles were calcined at 500°C for 1 h. The prepared samples were characterized respectively by XRD, SEM, FTIR, and UV-Visible analysis.	increasing precursor concentration showed an increase in the degree of crystallinity and an increase in crystal size. The average crystal size of the sample was calculated from the peak width using the Scherrer equation. The average sizes of crystallites found were 3.4 nm and 9.0 nm for the samples prepared with precursor concentrations of 0.01 and 0.1 mol, respectively.			
Sol-gel	La(OH) ₃ was dispersed in 40 ml of deionized water in a beaker. 0.1 M NaOH solution was added to the La(OH) ₃ solution and stirred using a magnetic stirrer to adjust the pH of the solution to about 10-11. To this basic solution, an amount of 10 vol% TEOS controlled with methanol was added dropwise with continuous stirring. The	The XRD pattern of the sample prepared by the sol-gel method and calcined at 400°C matched the monoclinic lanthanum hydroxide (LaOOH) pattern. Peak at 2θ = 26.6, 28.9, and 29.9 in the XRD pattern of samples	The sol-gel process is a highly flexible synthetic method with high level of processability, so that the resulting nanocomposite material can be fabricated into	Require long processing time and very high temperature	[19]

Table 1. Comparison of Methods Used in Synthesis La₂O₃ nanoparticle (continued)

Method	Synthesis procedure	Result	Advantages	Deficiency	Ref
Sol-gel	the solution was heated in an oil bath at 40°C for 2 hours. The gel was dried at 120°C and calcined at 400, 600, and 800 °C for 2 hours. The properties of the La ₂ O ₃ /SiO ₂ nanocomposite were compared with previously reported pure La ₂ O ₃ crystals.	calcined at 600°C indicate the evolution of hexagonal La ₂ O ₃ . When the calcination temperature reaches 800°C the characteristic diffraction peaks become very intense and well separated justifying the formation of hexagonal La ₂ O ₃ crystals.	various shapes including powders, rods, thin films, and others.		
Sono-chemical	The obtained lanthanum carbonate nanoparticles were calcined at 600°C for 2 hours to synthesize lanthanum oxide nanoparticles. The influence of several other parameters such as sonication time, calcination temperature, and surfactant. It was noted that 3 mL of polyethylene glycol (PEG) 600 as a surfactant was added to the lanthanum acetate solution.	Substances contained in La ₂ O ₃ were further examined using XPS. The binding energies obtained in the XPS analysis were corrected for the specimens with reference to C1 to 284.50 eV. The XPS spectrum of the product survey showed that there were no other metallic elements on the sample surface except La. That the binding energies La 3d _{5/2} dan La 3d _{3/2} are 834.71 and 851.47 eV, respectively.	This method does not require high temperatures or pressures.	Requires a high-power instrument	[20]

Table 1. Comparison of Methods Used in Synthesis La₂O₃ nanoparticle (continued)

Method	Synthesis procedure	Result	Advantages	Deficiency	Ref
		It can be seen that O1s are asymmetrical, indicating that two oxygen species are present in the adjacent region. The peak at about 529.92 eV can be indexed to O ₂ ⁻ in La ₂ O ₃ .			
Spray pyrolysis	[LaCl ₃ •7H ₂ O] solid particles with 99.5% purity. Pure H ₂ O ₂ analysis. Lanthanum chloride is dissolved in a certain concentration of hydrogen peroxide solution, the formation of a solution spray, in a homemade pyrolysis reaction. The development of the La ₂ O ₃ phase was observed using XRD on X'pert PRO DY2198 PANalytical with Cu Kα1 radiation and scanning speed of 10°/min. DTA was carried out in a differential thermal analyzer model STA 449F3 made by the NETZSCH Company. Approximately 68 mg of the lanthanum chloride sample was used for the DTA measurement. The lanthanum chloride sample was placed in an Al ₂ O ₃ crucible surrounded by N ₂ and O ₂ gases at a rate of 100 mL/min. Both heating	To determine the effect of the temperature of the pyrolysis reaction, the concentration of Lanthanum chloride was 0.52 mol/L, VLaCl ₃ : VH ₂ O ₂ =1, respectively at 600, 700, 800, and 900°C for the pyrolysis reaction. Conversion rates at 600, 700, 800, and 900°C were approximately 56.32, 75.35, 87.78, and 91.22%, respectively. The conversion rate of lanthanum chloride increases with increasing reaction temperature. The reason is that the pyrolysis reaction	This method does not harm the environment and can be applied to other rare earth chloride pyrolysis processes, aluminum chloride, cobalt chloride, nickel chloride, and others.	The method needs very high temperature	[21]

Table 1. Comparison of Methods Used in Synthesis La₂O₃ nanoparticle (continued)

Method	Synthesis procedure	Result	Advantages	Deficiency	Ref
	and cooling rates are 10/min	threshold energy of lanthanum chloride at more than the experimental temperature can be provided.			

Table 2. Plant materials, researcher, methods, and results of La₂O₃ green synthesis

Material	Research Group	Methods	Result	Ref
<i>Sesbania gradiflora</i> Leaves	Renjusha S	Eco-friendly	La ₂ O ₃ nanoparticles with single particle shape and size are spherical in size and below 100 nm based on scanning electron microscopy (SEM) analysis	[22]
<i>Juvenile maize roots</i>	Le Yue et al.	Lignin Synthesis	La ₂ O ₃ nanoparticles with NP and BP sizes of 80-100 nm and 1 μm	[23]
<i>Datura metel leaves</i>	R. Uma Maheswari et al.	Mediated Inorganic	La ₂ O ₃ nanoparticles with nanocrystal size 200 nm to 500 nm based on Transmission electron microscope (TEM) images	[24]
<i>Nothopanax scutellarium leaves</i>	Mustafa et al.	Two-phases system (n-hexane/water) with high-speed stirring	La ₂ O ₃ nanoparticles with a particle size of 84.3 nm based on Transmission electron microscopy (TEM)	[25]
<i>Physalis angulata leaf</i>	Sulaiman et al.	Eco-friendly	Single particle shape and size of La ₂ O ₃ nanoparticles measured using TEM are spherical with sizes ranging from 25-50 nm	[26]
<i>Andrographis paniculata leaves</i>	Muthulakshmi et al.	Hydrothermal at low temperature	La ₂ O ₃ nanoparticles with a particle size of 55 to 84 nm and have an average of 67 nm	[27]

4. Results and discussion

4.1 Method for forming La_2O_3 nanoparticles from raw material

4.1.1 Co-precipitation method

The co-precipitation method has several advantages, including simple process, low cost, high degree of crystallization, pure phase, and controllable powder particle size [28]. In this advantage, La_2O_3 nanoparticles are prepared by the co-precipitation method using lanthanum nitrate hexahydrate ($\text{La}(\text{NO}_3)_3 \cdot 6\text{H}_2\text{O}$) as a precursor and sodium hydroxide (NaOH) can act as a precipitating agent. The physical, chemical, morphological and optical characteristics of the La_2O_3 nanoparticles were characterized respectively by XRD, SEM, FTIR, UV-Visible DRS, and PL analysis tools. [14].

The XRD pattern of the uncalcined La_2O_3 nanoparticles contains several peaks as shown in **Fig 1(a)**. Extended intensity peaks exhibit polycrystalline properties and reduced size of La_2O_3 nanoparticles, in addition to extended intensity peaks, very weak intensity peaks were also observed in the XRD pattern which may appear due to the presence of hydroxides and carbonates in the uncalcined La_2O_3 nanoparticles. All identified La_2O_3 peaks are in accordance with the JCPDS file (50-6002) and are in accordance with previous reports [29,30]. **Fig 1(b)**. The matched linear equation data from the W-H plot were used to calculate the crystal size (using the intercept value) and the microstrain (slope) of the particles.

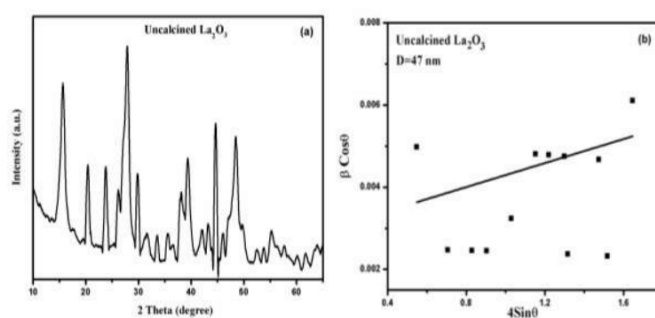


Figure 1. Results of structural analysis (a) XRD pattern (b) W-H Plot of uncalcined La_2O_3 nanoparticles. Image adapted from Ramjeyanti et al.[14].

The SEM micrograph obtained from the synthesis of La_2O_3 nanoparticles is shown in **Fig 2**. The surface of the uncalcined La_2O_3 nanoparticles is spherical with a uniform size distribution. In addition, some particle agglomeration was also observed in the SEM images. Due to the presence of particle agglomeration, the exact particle size value is not easy to calculate. The approximate value of the mean particle size was found to be 37 nm [14].

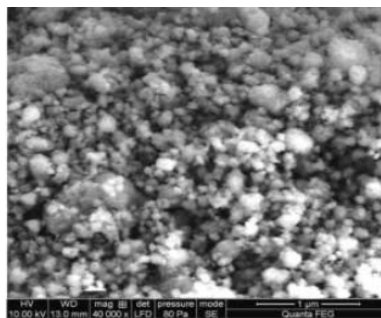


Figure 2. SEM image of the uncalcined La₂O₃ nanoparticles.

Image adapted from Ramjeyanti et al. [14].

Fig 3(a) shows that the reflectance spectrum of La₂O₃ nanoparticles is obtained in the wavelength range of 200-900 nm. The K-M plot is drawn between $(h\nu F(R))^{1/2}$ vs $h\nu$ as shown in **Fig 3(b)**. A straight line is drawn tangent to the point of interaction with the $h\nu$ axis giving an indirect energy bandgap of 5.35 eV [14].

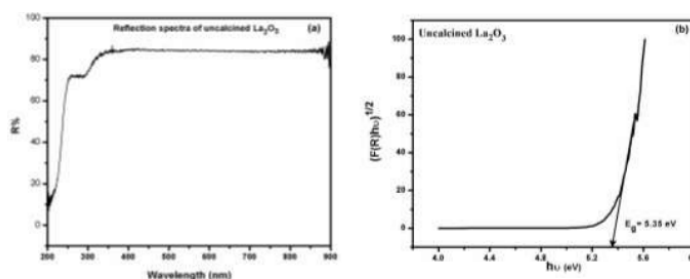


Figure 3. (a) room temperature optical reflectance spectrum and (b) K-M plot on La₂O₃ nanoparticles.

Image adapted from Ramjeyanti et al. [14].

4.1.2. Hydrothermal reaction

The hydrothermal reaction has been used as a relatively simple and strong method of synthesizing nanoparticles and nanorods/wires. Compared to other methods, the hydrothermal process has the following advantages: (a) effective control of particle size and shape; (b) shorter preparation time; (c) fewer impurities in the final product. So the hydrothermal method is widely used to prepare nanostructured materials [31-35].

The surfactant-assisted hydrothermal method to synthesize lanthanum oxide was the first to use the cationic surfactant CTAB as the templating agent and lanthanum chloride as the precursor. The obtained nanorods are small in diameter, and high aspect ratio (5–15 nm wide and 200–400 nm long). Meanwhile, a porous structure in lanthanum oxide was found, and this structure was still maintained after the removal of the surfactant by simple air calcination at 450°C [15].

X-ray diffraction measurements were carried out to determine the composition and phase structure of

the sample. Obtained samples with different shapes all giving a similar XRD pattern, a rod-like product is shown as an example. **Fig 4** is an XRD pattern of samples calcined for 2 hours at 450 and 850°C, respectively. **Fig 4(a)** shows the diffraction peaks of La_2O_3 and LaOCl , indicating the possible reaction of non-hydrolyzed lanthanum chloride. In **Fig 4(b)**, most of the peaks can be readily indexed as a hexagonal La_2O_3 structure (JCPDS card no. 73–2141). Strong and broad peaks indicate that the material has good crystallization and small size [15].

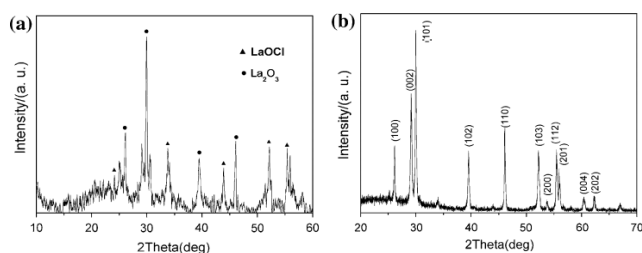


Figure 4. Typical XRD pattern of the synthesis product calcined at different temperatures. (a) 450 and (b) 850 °C. Image adapted from Sheng et al. [15].

Fig 5(a) shows a typical TEM image of the processed product obtained using 0.3 mL $\text{NH}_3\cdot\text{H}_2\text{O}$ (pH 8.5) the product mainly consists of La_2O_3 nanorods and nanorods with 5–15 nm in diameter and 200–400 nm in length. The SAED pattern (in **Fig 5(a)**) was recorded with the electron beam perpendicular to the long axis of the hexagonally structured La_2O_3 nanorod and the highly symmetrical dashed lattice in the ED pattern identifying the rod-like nature of La_2O_3 single crystals. When the amount of $\text{NH}_3\cdot\text{H}_2\text{O}$ was decreased from 0.3 to 0.1 mL (pH 6), while keeping other conditions constant as for La_2O_3 nanorods, the product was La_2O_3 nanoneedles, as shown in **Fig 5(b)**. As the amount of $\text{NH}_3\cdot\text{H}_2\text{O}$ from 0.3 to 0.6 mL (pH 9), increased from 0.3 to 0.6 mL (pH 9.0), the product morphology was parallel nanorods and bundled nanorods, as shown in **Fig 5 (c,d)**. Inset the ED pattern in **Fig 5(d)** corresponds to the La_2O_3 nanorod bundle.

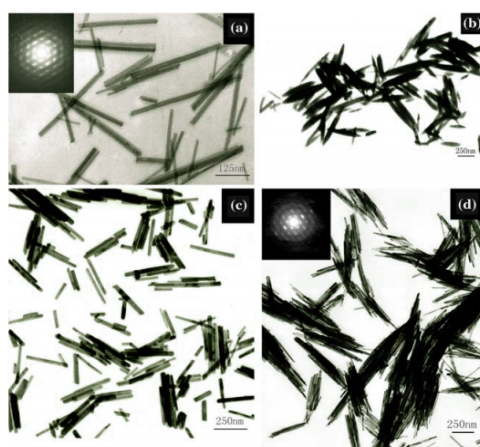


Figure 5. TEM images of samples at different pH values. (a) pH 8,5 (b) pH 6,0 (c) pH 9,0 (d) pH 10,0.

Image adapted from Jie Sheng et al., 2007 [15].

Fig 6(a) at 40°C, La_2O_3 is a uniformly distributed nanorod with a length of about 120 nm. When the reaction temperature was kept at 60°C (**Fig 6(b)**), La_2O_3 nanorods were observed with a length of about 200 nm. As the reaction temperature increased to 80°C (**Fig 6(a)**), the nanorod length became longer. The average length can reach 400 nm while the diameter does not change significantly.

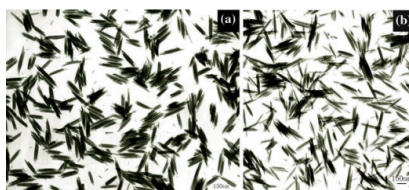


Figure 6. TEM image samples obtained at different temperatures. (a) 40 and (b) 60 °C. Image adapted from Jie Sheng et al., 2007 [15].

Fig 7 shows an image of the La_2O_3 nanorod made with different reaction times. The results showed that the length of the nanorods grew longer with increasing reaction time. At 8 h (**Fig 7(a)**), a rod with a length of 85 nm and a width of 5 nm was obtained. When the time was increased to 12 h (**Fig 7(b)**), the length of the nanorods became 120 nm. Meanwhile, when the time reached 24 hours, the length changed to 200–400 nm (**Fig 7(a)**). Thus, reaction time also plays an important role in influencing the nanorod length [15].

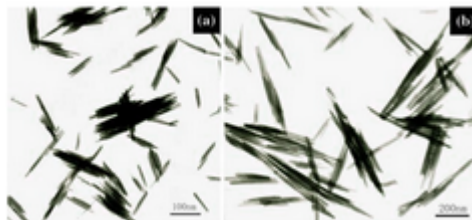


Figure 7. TEM images of samples obtained at different reaction times. (a) 8 and (b) 12 hours. Image adapted from Jie Sheng et al., 2007 [15].

4.1.3. Solution combustion

The solution combustion method meets the demand for higher integration density in microelectronics, MOSFET scaling is becoming more aggressive. In the future, a leading manufacturer of integrated circuits recently announced to introduce hafnium and lanthanum-based high- κ dielectrics in the next new generation of CMOS [36].

Bikshalu et al. have reported the synthesis of La_2O_3 nanoparticles using the Pechini Method for Future CMOS Applications [16] and Pathan et al. have reported the synthesis of La_2O_3 nanoparticles using glutamic acid and Propylene glycol for Future CMOS Applications [26]. This method used Lanthanum Nitrate mixing with Acetamide as fuel [16].

Fig 8, EDAX La_2O_3 spectrum showing peaks for lanthanum and elemental oxygen indicating the

formation of La_2O_3 nanoparticles. The peak indexing of these elements is oxygen 0.52 keV and lanthanum 4.71 keV. The mass percentage composition of these elements is 35.15% of oxygen and 64.42% of lanthanum. The observed composition corresponds to the theoretically calculated composition.

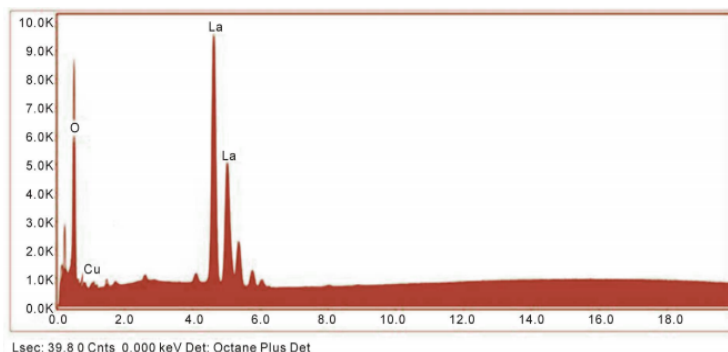


Figure 8. EDAX Spectrum of La_2O_3 Nanoparticles. Image adapted from Amanullakhan A. et al., 2018 [16].

TEM analysis showed samples agglomerated in the nano range. **Fig 9** shows a TEM micrograph of a sample synthesized using this method. From the TEM analysis, it was found that the sample particles were not well in the crystal due to severe agglomeration. But the particles are well below the nanometer range to conclude that the particles obtained are Nanoparticles [16].

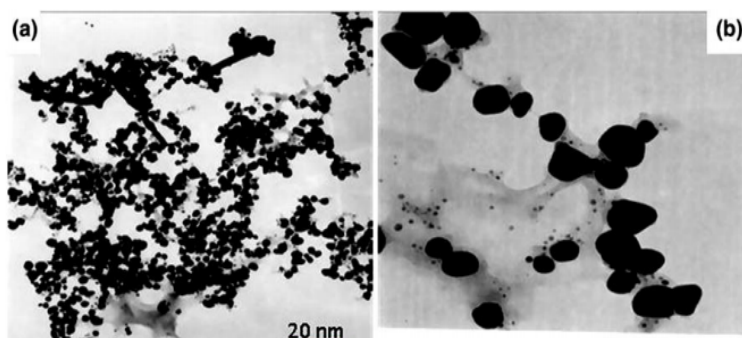


Figure 9. (a) and (b) TEM images of La_2O_3 nanoparticles synthesized by retaining using $\Psi = 1$. Image adapted from Amanullakhan A. et al., 2018 [16].

4.1.4. Thermal decomposition

Lanthanum oxide nanoparticles were obtained by calcining carbonate precursors in a furnace at 650°C for 3 hours under a static air atmosphere. SEM images of the fabricated metal oxide particles are shown in **Fig 10**. As expected, the oxide particles display a globular morphology.

The average size of lanthanum oxide and copper oxide nanoparticles determined by SEM images was between 35 and 30 nm, respectively. The XRD technique was also used to characterize the resulting metal oxide nanoparticles [17].

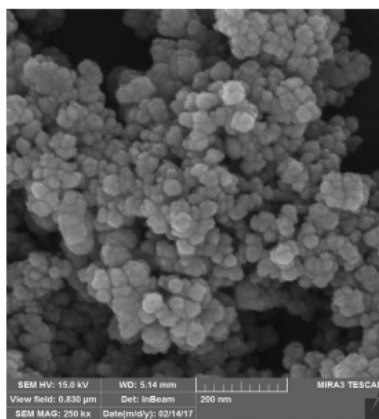


Figure 10. SEM image of nano-sized La_2O_3 NPs synthesized by precursor calcination. Image adapted from Hossein Momenizadeh. et al., 2018 [17]

4.1.5. Reflux

The prepared samples show a Plate-like morphology. It proves that the sample prepared with a higher concentration of 0.1 mol of precursor indicates the plate being formed with the non-uniform distribution. SEM images are presented in **Fig 11(a)** corresponding samples were prepared with different precursor concentrations of 0.01 mol. The morphology is like a nanoplate which has a smoother surface with a thickness ranging from 50–80 nm.

The morphology of the sample prepared with the 0.1 mol higher precursor concentration is shown in **Fig 11(b)**. It proves that more precursors act as a feed source for plate structure growth. It can be concluded that the plate-like structure is still in formation which is evident from the incomplete structure seen in the SEM images [18].

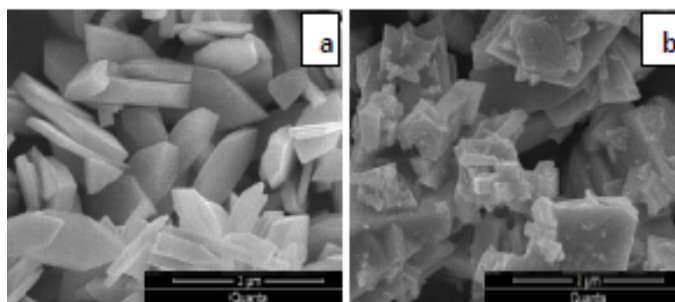


Figure 11. SEM image of a La_2O_3 sample prepared with precursor concentrations of (a) 0.01 mol and (b) 0.1 mol. Image adapted from Kathikeyan et al. [37].

4.1.6. Sol-gel

All chemicals are of analytical grade and are used without further purification. $\text{La}_2\text{O}_3/\text{SiO}_2$ nanocomposites were prepared using the sol-gel process [38]. The XRD pattern of the sample prepared by the sol-gel method and calcined at 400, 600, 800 °C and pure La_2O_3 is shown in **Fig 12**. The XRD

pattern of the sample calcined at 400 °C (**Fig 12(a)**) corresponds to the monoclinic XRD pattern. lanthanum hydroxide oxide (LaOOH). Peaks at $2\theta = 26.6, 28.9,$ and 29.9° in the XRD pattern of samples calcined at 600°C (**Fig 12(b)**) indicate the evolution of hexagonal La_2O_3 . When the calcination temperature reaches 800°C (**Fig 12(c)**) the characteristic diffraction peaks become very intense and well separated justifying the formation of hexagonal La_2O_3 crystals [19].

Peaks correspond to SiO_2 at $2\theta = 21.0^\circ, 21.9^\circ, 28.0, 31.0^\circ$. In addition, several other conditions were examined to investigate the morphology of the products and compare them with each other. The relationship between the average particle size of La_2O_3 and the calcination temperature is plotted in **Fig 12** when the calcination time is 2 hours. The results showed that the average particle size increased with increasing calcination temperature. It grows slowly at lower temperatures and increases very rapidly when the temperature is above 750°C. **Fig 12(a-d)** shows SEM images of lanthanum oxide nanoparticles calcined at 650, 700, 750, and 800 °C for 2 h respectively. Quasi-spherical nanoparticles were observed when the calcination temperature was below 700°C. At 750°C, the particles begin to agglomerate and enlarge. When the temperature reaches 800°C, all the particles have been completely sintered together leading to the formation of large particles [39]. The results showed that the size of the La_2O_3 nanoparticles depends on the calcination temperature. By increasing the calcination temperature, larger La_2O_3 nanoparticles were prepared [20], in the diffraction pattern (**Fig 12(c)**) confirming the formation of La_2O_3 in the SiO_2 matrix [40]. The slight shift and decrease in the intensity of the diffraction peak compared to pure La_2O_3 (**Fig 12(d)**) may be due to the influence of SiO_2 nanoparticles in the vicinity of La_2O_3 [41]. Thus the mechanism of the $\text{La}(\text{OH})_3$ dehydration process that leads to the formation of $\text{La}_2\text{O}_3/\text{SiO}_2$ nanocomposites can be explained by the following equation [42].

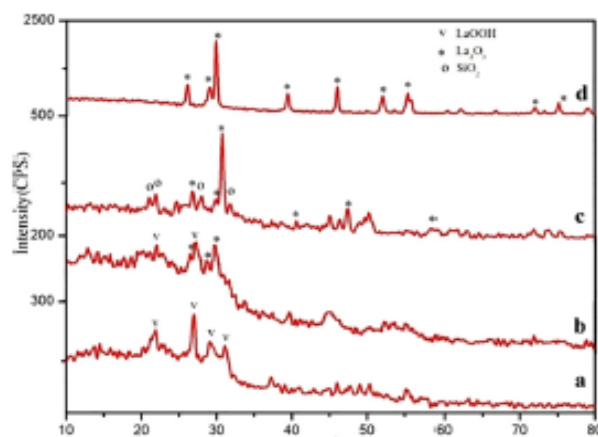


Figure 12. XRD pattern of the sample prepared by the sol-gel method and calcined at (a) 400, (b) 600, and (c) 800 °C, (d) pure La_2O_3 . Image adapted from Moothedan and Sherry [40].

4.1.7 Sono-chemical

Among the many available synthetic techniques, the sonochemical method has proven to be a versatile technique for the preparation of complex structures with different morphologies, such as nanorods [43], core-shell nanorods [44], nanospindles [45], and dendritic structures [46], and this method does not require high temperatures or pressures [20].

TEM images of the products are shown in **Fig 13**. **Fig 13 (a-c)** shows TEM images of $\text{La}_2(\text{CO}_3)_3$ (sample no. 2), $\text{La}(\text{OH})_3$ (sample no. 5), and La_2O_3 (sample no.7) nanoparticles, respectively. The size of the $\text{La}_2(\text{CO}_3)_3$ nanoparticles obtained from the XRD diffraction pattern is very consistent with the TEM study which shows a size of 25–35nm for sample no.2 with a quasi-spherical shape, also the observed particles are agglomerated (**Fig 13(a)**). **Fig 13(b)** shows a TEM image of $\text{La}(\text{OH})_3$ nanoparticles, sample no. 5. The particle size of $\text{La}(\text{OH})_3$ is about 16–20 nm. According to the TEM image of La_2O_3 nanoparticles, sample no. 7, La_2O_3 particles are about 30 nm in size with a spherical shape **Fig 13(c)**.

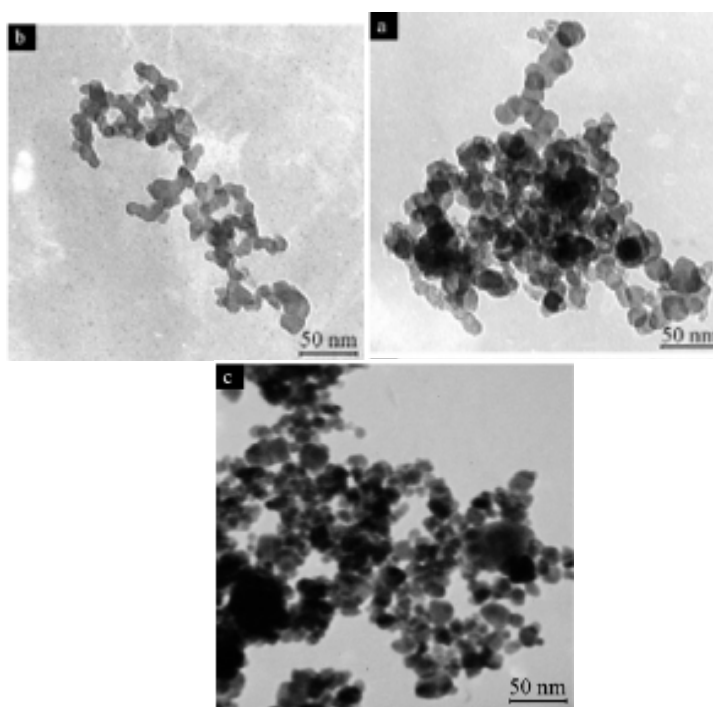


Figure 13. TEM image of (a) sample no. 2, (b) sample no. 5, and (c) sample no. 7.

Image adapted from Salavati-Niasari et al. [20].

In addition, several other conditions were examined to improve the morphology of the products and compare them with each other. The relationship between the average particle size of La_2O_3 and the calcination temperature is plotted in **Fig .14** when the calcination time is 2 hours. The results showed that the average particle size increased with the calcination temperature. It grows slowly at lower temperatures and increases very rapidly when the temperature is above 750°C . **Figs. 15(a-d)** show SEM images of lanthanum oxide nanoparticles calcined at 650 , 700 , 750 , and 800°C for 2 hours, respectively.

Quasi-spherical nanoparticles were observed at calcination temperatures below 700°C. At 750°C, the particles begin to agglomerate and enlarge. When the temperature reaches 800°C, all the particles have been completely separated together leading to the formation of large particles [39]. The results showed that the size of the La₂O₃ nanoparticles depended on the calcination temperature. By increasing the calcination temperature, larger La₂O₃ nanoparticles were prepared [20].

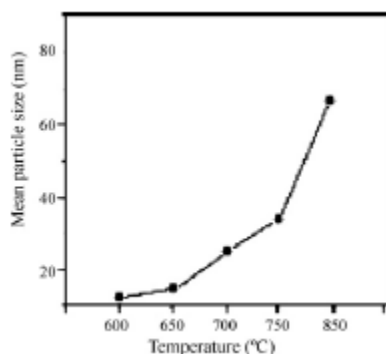


Figure 14. The average particle size of La₂O₃ nanoparticles as a function of calcination temperature.

Image adapted from Salavati-Niasari et al.[20].

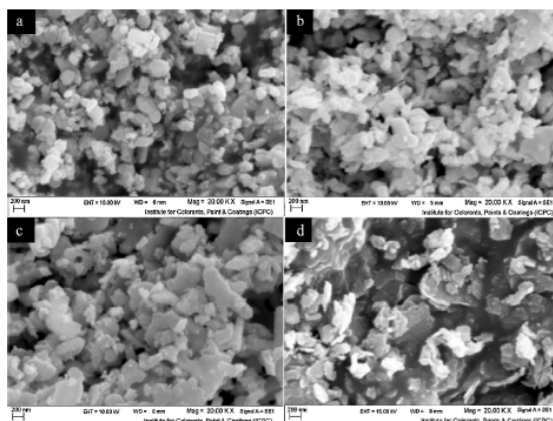
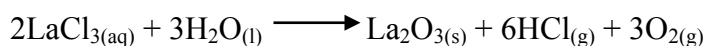


Figure 15. SEM image of La₂O₃ nanoparticles: (a) sample no. 8, (b) sample no. 9, (c) sample no. 10, and (d) sample no. 11. Image adapted from Salavati-Niasari et al.[20].

4.1.8 Spray pyrolysis

Hydrogen peroxide is a strong oxidant, to combine in the solution of lanthanum chloride excess hydrogen peroxide can effectively promote the resulting oxide process, and excess hydrogen peroxide decomposes into oxygen at high temperature, which has no pollution with the resulting lanthanum oxide. The process equations for the pyrolysis of lanthanum chloride in solution or hydrogen peroxide are presented, respectively:



In the hydrogen peroxide system of direct lanthanum chloride solution, the pyrolysis reaction temperature is significantly lower. XRD results show that the product is a mixture of LaCl₃ and La₂O₃.

That is, the direct transformation of lanthanum chloride to lanthanum oxide is still a challenging task. It was found from the DTA thermogram that a clear and weightless endothermic peak is located in the single-phase region at temperatures above 1000°C, according to the thermodynamic calculations shown in Fig 16, it is known that lanthanum oxide is produced at temperatures above up to 1000°C [21].

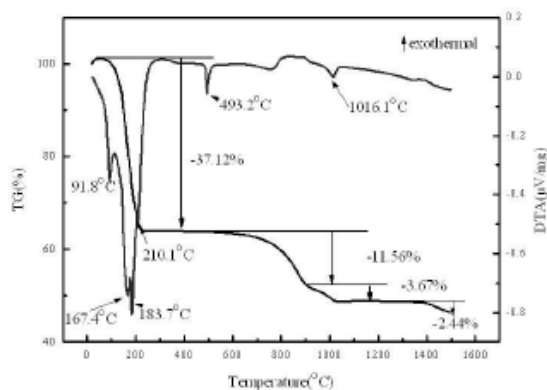


Figure 16. DTA lanthanum chloride thermogram at a heating rate of 10°C/min.

Image adapted from Wang et al. [21].

4.2 Method for extracting La₂O₃ NPs from plant sources

Green synthesis of nanoparticles is the best choice because of its outstanding advantages such as being one-pot, non-toxic, bio-compatible, and requires less energy [1, 4, 5]. The use of plant extracts in the synthesis of La₂O₃ nanoparticles that are environmentally friendly, simple, fast, and takes place in one step, biomolecules found in various parts of plants such as amino acids, proteins, tannins, enzymes, saponins, phenols, vitamins, sugars, and flavonoids have medicinal and medicinal importance environmentally friendly [35]. The choice of plants depends on the phytochemicals present in them and their medicinal importance, after the selection of plants, certain parts are selected (fruit, flowers, leaves, bark, latex, and roots), washed several times with distilled water, and crushed or cut into small pieces and boiled to get the extract.

The plant extract was filtered through filter paper and a solution of lanthanum salt was added while stirring continuously at the desired temperature, to maintain an alkaline pH, an alkaline solution (NaOH) was added. In the alkaline medium, acidic protons are abstracted and phytochemicals are activated to react with lanthanum salts, after bio-reduction to produce La₂O₃ nanoparticles. The prepared nanoparticles were separated by filtration and washed with distilled water, dried and calcined, characterized, and finally used for the desired application [26].

4.2.1 *Sesbania grandiflora* leaves as a source of La₂O₃

Sesbania grandiflora is a small, erect, fast-growing, and sparsely branched tree belonging to the Leguminosae family. This plant comes from tropical Asia and is widespread in Malaysia, Indonesia, the

Philippines, and India. All parts of *S. grandiflora* have been used empirically as traditional medicine in traditional medicine to treat various diseases such as inflammation of the mucous membranes of the nose, dysentery, fever, headache, smallpox, sore throat, and stomatitis [46]. These chemical constituents are well known for their potential health benefits and have been reported to possess valuable biological activities such as antibacterial, antifungal [33], antiurolytic antioxidant, anticonvulsant, anxiolytic, and hepatoprotective properties.

An aqueous extract of *S. grandiflora* was prepared using freshly collected leaves. Leaves were surface cleaned with running tap water, followed by double sterilized distilled water, and then shade dried for 5 days to remove moisture completely. The fine powder is obtained from dried leaves that are mashed using a kitchen blender. Leaf powder (10 g) was taken and mixed with 100 ml of Milli Q water and stored in a water bath at 60°C for 10 minutes. The extract was filtered through a nylon net (0.2 μ m) and followed by Whatman filter paper. The filtered extract was stored at 4°C for further study [34].

4.2.2 Juvenile maize as a source of La₂O₃

Corn (*Zea mays L.*) is one of the staple crops with an annual production of around 1.4 billion tonnes in 2017 (www.fao.org). Due to its subtropical origin, maize cultivation in the Northern Hemisphere is somewhat challenging due to the cool spring temperatures [47]. These cold temperatures, averaging 17°C during the day and 12°C at night, inhibit plant development and ultimately result in crop loss [48-50].

Low temperature affects root system growth, dry weight, and root branching of seedlings are much less below 15°C [51]. Furthermore, root length is more affected by suboptimal temperature than root dry weight [52] and a shorter root system limits the absorption of several nutrients, including phosphorus [53], potassium [54], and nitrogen [55].

4.2.3 *Datura metel* as a source of La₂O₃ nanoparticles

Datura metel leaf extract as a medicinal plant to synthesize inorganic rare-earth La₂O₃ nanocrystals. *Datura metel* (*Solanaceae*) is a medicinal plant that has been reported primarily for its healing properties. In addition, the leaf extract contains phytochemical constituents such as alkaloids, terpenoids, flavonoids, steroids, anthraquinones, glycosides, and tannins [24].

4.2.4 *Nothopanax scutellarium* as a source of La₂O₃ nanoparticles

Nothopanax scutellarium is an ornamental or hedge plant that grows wild in fields and river banks. In previous studies, this plant is a local drug for hair growth that contains about 11% of alkaloids and other secondary metabolites such as flavonoids, saponins, and tannins. Alkaloids function as hydrolyzing

agents (source of weak base OH⁻). Meanwhile, other secondary metabolites such as saponins and tannins act as capping agents for the growth of La₂O₃ nanoparticles [47].

4.2.5 *Physalis angulata* as a source of La₂O₃

The leaves of *Physalis angulata* are *Solanaceae*. Cultivated by the Sundanese, West Java, Indonesia as a medicinal plant and the ethanolic extract of its leaves contains about 2% alkaloid compounds and other compounds such as flavonoids, saponins, cyanides, phytates, and tannins [56-58]. Crude methanol extract of *Physalis angulata* leaves also contains alkaloids, saponins, and steroids. Alkaloid compounds in *Physalis angulata* can be used as a source of weak bases, while other secondary metabolites such as saponins and flavonoids can act as stabilizers [59] in the formation of La₂O₃ nanoparticles. A phytochemical test was used to identify the presence of alkaloids, flavonoids, and saponins in the leaf extract of *Physalis angulata* [26].

Identification of the functional group of La₂O₃ nanoparticles was analyzed using FTIR spectrometry. Fig 17 shows the spectrum of PALE FTIR and the formed La₂O₃ nanoparticles. The PALE FTIR spectrum shows C-N vibrations at 1402 cm⁻¹ which indicates the presence of alkaloids that act as weak bases in the formation of La(OH)₃. The phytochemical test results also confirmed the presence of alkaloid compounds and other secondary metabolites such as saponins, flavonoids, and polyphenols contained in PALE water. Alkaloids act as weak bases while saponins, flavonoids, and polyphenols act as stabilizing agents [59] in the formation of La₂O₃ NPs. The La₂O₃ spectrum (red line) reported that La₂O₃ was successfully synthesized using PALE as indicated by the La-O interactions occurring at vibrations of 400 cm⁻¹ and 454 cm⁻¹, which ranged from 400-660 cm⁻¹ according to the literature [60,61].

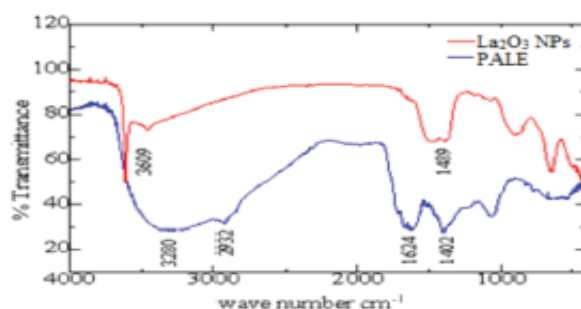


Figure 17. FTIR spectra of PALE (blue line) and calcined La₂O₃ NPs at 700 °C for 2 hours (red line). Image adapted from Sulaiman N., Y. Yulizar, and D. O. B. Apriandanu, 2018 [61].

4.2.6 *Andrographis paniculata* leaves as a source of La₂O₃

Green method of synthesis of La₂O₃ nanoparticles using *Andrographis paniculata* leaf extract. The fresh leaves collected were washed three times with ultrapure water to remove dust and dirt. *Andrographis paniculata* leaves were cut into small pieces and dried at room temperature for about 15 days under dust-

free conditions. Then the dried leaves were taken in a soxhlet apparatus under running water, and about 25 mL of ethanol was further added to this mixture, which was boiled for 30 minutes at 60°C. The obtained ethanolic solution of *Andrographis paniculata* extract was cooled and filtered through Whatman No.1 filter paper. The filtrate extract was collected, and stored in a refrigerator at 4°C. An aqueous solution of 0.1 mol/L lanthanum chloride [LaCl₃·7H₂O] was mixed with 20 mL of *Andrographis paniculata* leaf extract and added to 1.0 mL of [BMIM PF6] IL solution while stirring for 3 hours at room temperature. The reaction mixture was filtered and separated by centrifugation at 1000 rpm for 10 min. After that, the resulting sample was filtered, washed with distilled water, and dried in an air oven at 100°C. This powder sample was calcined in a muffle furnace for 5 hours at 650°C to obtain La₂O₃ nanoparticles [62].

Conclusion

La₂O₃ synthesis can be carried out by several methods, such as co-precipitation, hydrothermal reaction, solution combustion, thermal decomposition, reflux, sol-gel, sonochemical, and spray pyrolysis. From these methods, the most efficient way to synthesize La₂O₃ is the hydrothermal method, because this method requires high temperatures but good results, lower costs, relatively uniform particle size, and produces homogeneous crystals. The most potential plant is *Physalis angulata* because there are many plants in Indonesia, the synthesis of good nanoparticles produces a size of 25-50 nm, and the compounds contained can also be used for the pharmaceutical field.

Acknowledgments

We acknowledged Bangdos Universitas Pendidikan Indonesia.

References

- [1] N. K. Mogha, Sahu, V., Sharma, M., Sharma, R. K., & Masram, D. T, Sensitive and reliable ascorbic acid sensing by lanthanum oxide/reduced graphene oxide nanocomposite. *Applied Biochemistry and Biotechnology*. 174, 3: 1010-1020 (2014).
- [2] S. V. Yap, R. M. Ranson, W. M. Cranton and D. Koutsogeorgis, Decay time characteristics of La₂O₃S:Eu and La₂O₃S:Tb for use within an optical sensor for human skin temperature measurement. *Applied Optics*. 47, 27: 4895–4899 (2008).
- [3] B. Balusamy, G. K. Yamuna, S. Anitha, C. Gopalakrishnan, S. S. Murugan and T. S. Kumaravel, Characterization and bacterial toxicity of lanthanum oxide bulk and nanoparticles, *J. Rare Earths*. 30, 12: 1298–1302 (2012).
- [4] J. Liu, W. Mei, Y. Li, E. Wang, L. Ji and P. Tao, Antiviral activity of mixed valence rare earth

- borotungstate heteropoly blues against influenza virus in mice. *Antiviral Chemistry and Chemotherapy*. 11, 6: 367–372 (2000).
- [5] A. Guha and A. Basu, Role of rare earth oxide nanoparticles (CeO_2 and La_2O_3) in suppressing the photobleaching of Fluorescent organic dyes. *Journal of fluorescence*. 24, 3: 683–687 (2014).
- [6] N. Zhang, Y. Ran, Z. Libin, G. Guanhua, S. Rongrong, Q. Guanzhou and L. Xiaohe, Lanthanide hydroxide nanorods and their thermal decomposition to lanthanide oxide nanorods. *Materials Chemistry and Physics*. 114: 160–167 (2009).
- [7] A. Corti, Mannarino, C., Mazza, R., Angelone, T., Longhi, R., & Tota, B, Chromogranin A N-terminal fragments vasostatin-1 and the synthetic CGA 7–57 peptide act as cardiostatins on the isolated working frog heart. *General and Comparative Endocrinology*. 136, 2: 217-224 (2004).
- [8] J. Fang, Saunders, M., Guo, Y., Lu, G., Raston, C. L., & Iyer, K. S, Green light-emitting LaPO_4 : Ce^{3+} : Tb^{3+} koosh nanoballs assembled by p-sulfonato-calix [6] arene coated superparamagnetic Fe_3O_4 . *Chemical Communications*. 46, 18: 3074-3076 (2010).
- [9] T. H. A. Alabri, Al Musalami, A. H. S., Hossain, M. A., Weli, A. M., & Al-Riyami, Q, Comparative study of phytochemical screening, antioxidant and antimicrobial capacities of fresh and dry leaves crude plant extracts of *Datura metel* L. *Journal of King Saud University-Science*. 26, 3: 237-243 (2014).
- [10] H. Zhang, Ma X., Ji Y., Xu J., Yang D., Single crystalline CdS nanorods fabricated by a novel hydrothermal method. *Chemical Physics Letters*. 377, 5-6: 654-657 (2003).
- [11] H. Zhang, Ji Y., Ma X., Xu J., Yang D., Long Bi_2S_3 nanowires prepared by a simple hydrothermal method. *Nanotechnology*. 14, 9: 974 (2003).
- [12] L. Vayssieres, Growth of arrayed nanorods and nanowires of ZnO from aqueous solutions. *Advanced Materials*. 15, 5: 464-466 (2003).
- [13] H. Doweidar, & Saddeek, Y. B. Effect of La_2O_3 on the structure of lead borate glasses. *Journal of Non-crystalline Solids*. 356, 28-30: 1452-1457 (2010).
- [14] N. Ramjeyanthi, Alagar M, Muthuraman D., Synthesis structural and optical characterization of uncalcined lanthanum oxide nanoparticles by co-precipitation method. *Int. J. Interdisciplinary Res. Innov.* 6, 3:389-395 (2018).
- [15] J. Sheng, Zhang S, Lv S, Sun W, Surfactant-assisted synthesis and characterization of lanthanum oxide nanostructures. *Journal of Materials Science*. 42, 23: 9565-9571 (2007).
- [16] A. A. Pathan, Desai K. R., Vajapara S., Bhasin C. P., Conditional optimization of solution combustion synthesis for pioneered La_2O_3 nanostructures to application as future CMOS and NVMS generations. *Advances in Nanoparticles*. 7, 1: 28-35 (2018).
- [17] H. M. Pandas, Fazli M., Preparation and application of La_2O_3 and CuO nano particles as catalysts

- for ammonium perchlorate thermal decomposition. *Propellants, Explosives, Pyrotechnics*. 11:1096-104 (2018).
- [18] S. Karthikeyan, A. D. Raj, A. Irudayaraj, & R. L. Josephine, Effect of precursor concentration on the properties of lanthanum oxide nanostructures. 4390-4394 (2015).
- [19] M. Moothedan, & K. B. Sherly, Synthesis and characterization of low moisture permeation lanthanum oxide/silica nanocomposite. *Materials Today: Proceedings*. 25: 178-182 (2020).
- [20] M. Salavati-Niasari, G. Hosseinzadeh, & F. Davar, Synthesis of lanthanum carbonate nanoparticles via sonochemical method for preparation of lanthanum hydroxide and lanthanum oxide nanoparticles. *Journal of Alloys and Compounds*. 509, 1: 134-140 (2011).
- [21] W. A. N. G. Zhenfeng, Wenyuan, W. U., Xue, B. I. A. N., & Shoufeng, X. U. E., Synthesis of lanthanum oxide using hydrogen peroxide as auxiliary reagent by spray pyrolysis method. *Advanced Materials Research*. 1081. (2014).
- [22] S. Renjusha, Eco-friendly method for synthesis of La_2O_3 nanoparticles using *Sesbania grandiflora* leaf extract and its antibacterial studies.
- [23] L. Yue, Chen F, Yu K, Xiao Z, Yu X, Wang Z, Xing B, Early development of apoplastic barriers and molecular mechanisms in juvenile maize roots in response to La_2O_3 nanoparticles. *Science of The Total Environment*. 653: 675-683 (2019)
- [24] R. U. Maheswari, Yuvakkumar R., Ravi G., Hong S. I., Organic *Datura metel* leaf extract mediated inorganic rare earth La_2O_3 nanocrystals formation. *Journal of Nanoscience and Nanotechnology*. 19, 7: 4033-4038 (2019).
- [25] K. Mustofa, Yulizar, Y., Saefumillah, A., & Apriandanu, D. O. B. (2020, July). La_2O_3 nanoparticles formation using *Nothopanax scutellarium* leaf extract in two-phase system and photocatalytic activity under UV light irradiation. In *IOP Conference Series: Materials Science and Engineering* (902, 1, p. 012018). IOP Publishing.
- [26] N. Sulaiman, Yulizar, Y., & Apriandanu, D. O. B., Eco-friendly method for synthesis of La_2O_3 nanoparticles using *Physalis angulata* leaf extract. In *AIP Conference Proceedings* (2023, 1, p. 020105). AIP Publishing LLC (2018).
- [27] I. P. Sari & Y. Yulizar, Green synthesis of magnetite (Fe_3O_4) nanoparticles using *Graptophyllum pictum* leaf aqueous extract. *IOP Conf. Ser. Mater. Sci. Eng.* 012014: 191 (2017).
- [28] J. Luo, Chen, J., Li, W., Huang, Z., & Chen, C, Temperature effect on hydroxyapatite preparation by co-precipitation method under carbamide influence. In *MATEC Web of Conferences* (Vol. 26, p. 01007). *EDP Sciences* (2015).
- [29] A. Ezhilarasi, Vijaya J J, Kaviyarasu K, Maaza M, Ayeshamariam A and Kennedy L J. Green synthesis of NiO nanoparticles using *Moringa oleifera* extract and their biomedical applications:

- Cytotoxicity effect of nanoparticles against HT-29 cancer cells. *Photochem. Photobiol.* 164: 352-360 (2016).
- [30] S. Renjusha, Eco-friendly method for synthesis of La_2O_3 nanoparticles using *Sesbania grandiflora* leaf extract and its antibacterial studies.
- [31] Q. Yang, Tang K, Wang C, Qian Y, Zhang S., PVA-assisted synthesis and characterization of CdSe and CdTe nanowires. *The Journal of Physical Chemistry B.* 106, 36: 9227-9230 (2002).
- [32] J. H. Zhan, Yang X. G., Wang D. W., Li S. D., Xie Y., Xia Y., Qian Y, Polymer controlled growth of CdS nanowires. *Advanced Materials.* 12, 18: 1348-1351 (2000).
- [33] N. Hasan , H. Osman , S. Mohamad , W. K. Chong , K. Awang , A. S. M. Zahariluddin, The chemical components of *Sesbania grandiflora* root and their antituberculosis activity. 5: 882-889 (2012).
- [34] J. Das, Das M. P., Velusamy P., *Sesbania grandiflora* leaf extract mediated green synthesis of antibacterial silver nanoparticles against selected human pathogens. *Spectrochimica Acta Part A: Molecular and Biomolecular Spectroscopy.* 104: 265-270 (2013).
- [35] H. Dabbane, Ghotekar S, Tambade P, Medhane V, Plant mediated green synthesis of lanthanum oxide (La_2O_3) nanoparticles: A review. *Asian Journal of Nanosciences and Materials.* 3, 4:291-299 (2020).
- [36] Pechini, M. P. USA Patent, No. 3.330. 697 (1967).
- [37] S. Karthikeyan, A. Dhayal Raj, A. Albert Irudayaraj, D. Magimai Antoniraj, Effect of temperature on the properties of La_2O_3 nanostructures. *Science Direct.* 2: 1021-1025 (2015).
- [38] S. H. Joo, J. Y. Park, C. K. Tsung, Y. Yamada, P. Yang, & G. A. Somorjai, Thermally stable Pt/mesoporous silica core-shell nanocatalysts for high-temperature reactions. *Nature Materials.* 8, 2: 126-131 (2009).
- [39] X. Wang, M. Wang, H. Song, & B. Ding, A simple sol-gel technique for preparing lanthanum oxide nanopowders. *Materials Letters.* 60, 17-18: 2261-2265 (2006).
- [40] M. Moothedan, & K. B. Sherly, Synthesis, characterization and sorption studies of nano lanthanum oxide. *Journal of Water Process Engineering.* 9: 29-37 (2016).
- [41] A. Neumann, & D. Walter, The thermal transformation from lanthanum hydroxide to lanthanum hydroxide oxide. *Thermochimica Acta.* 445, 2: 200-204 (2006).
- [42] L. Qiu, V. G. Pol, J. Calderon-Moreno, & A. Gedanken, Synthesis of tin nanorods via a sonochemical method combined with a polyol process. *Ultrasonics Sonochemistry.* 12, 4: 243-247 (2005).
- [43] L. Zhu, X. Liu, Q. Li, S. Zhang, J. Meng, & X. Cao., Facile sonochemical synthesis of CePO_4 : Tb/ LaPO_4 core/shell nanorods with highly improved photoluminescent properties.

- Nanotechnology*. 17: 4217–4222 (2006).
- [44] J. Geng, J.J. Zhu, D.J. Lu, & H.Y. Hollow, PbWO₄ nanospindles via a facile sonochemical route. *Chen, Inorg. Chem.* 45: 8403–8407 (2006).
- [45] J. Geng, Y. Lv, D. Lu, & J. J. Zhu, Sonochemical synthesis of PbWO₄ crystals with dendritic, flowery and star-like structures. *Nanotechnology*. 17, 10: 2614 (2006).
- [46] Farooq M, Aziz T, Wahid A, Lee D-J, Siddique K. H. M., Chilling tolerance in maize: agronomic and physiological approaches. *Crop and Pasture Science*. 60, 6: 501–516 (2009).
- [47] J. Leipner, Stamp P, Fracheboud Y, Artificially increased ascorbate content affects zeaxanthin formation but not thermal energy dissipation or degradation of antioxidants during cold-induced photooxidative stress in maize leaves. *Planta*. 210: 964–969 (2000).
- [48] J. Leipner and Stam Peter. Chilling stress in maize seedlings. In *Handbook of Maize: Its Biology*. Springer, New York, NY. p. 291-310 (2009).
- [49] A. Sobkowiak, Jończyk M., Adamczyk J., Szczepanik J., Solecka D., Kuciara I., Molecular foundations of chilling-tolerance of modern maize. *BMC Genomics*.17: 125 (2016).
- [50] H. W. Cutforth, Shaykewich C. F., Cho C. M., Effect of soil water and temperature on corn (*Zea mays L.*) root growth during emergence. *Canadian Journal of Soil Science*. 66, 1: 51–58 (1986).
- [51] T. C. Kaspar, Bland W. L., Soil temperature and root growth. *Soil Science*. 154, 4: 290–299 (1992). doi: 10.1097/00010694-199210000-00005
- [52] A. D. Mackay, Barber S. A., Soil temperature effects on root-growth and phosphorus uptake by corn. *Soil Science Society of America Journal*. 48, 4: 818–823 (1984).
- [53] D. Steffens, Root system and potassium exploitation. Nutrient balances and the need for potassium. 97-108 (1986).
- [54] V. G. Shinde, V. B. Gaikwad, M. K. Deore, Synthesis of Lanthanum Oxide (La₂O₃) Nanoparticles by Hydrothermal method and studies it's Physical Properties. *International Journal of Chemical and Physical Sciences*. 7: 669-674 (2018).
- [55] W.L. Pan, W. A. Jackson, and R. H. Moll, Nitrate uptake and partitioning by corn (*Zea mays L.*) root systems and associated morphological differences among genotypes and stages of root development. *Journal of Experimental Botany* 36, 1341–1351 (1985). doi: 10.1093/jxb/36.9.1341
- [56] K. Roosita, C. M. Kusharto, M. Sekiyama, Y. Fachrurozi, R. Ohtsuka. *Journal of ethnopharmacology*. 115, 1: 72-81 (2008).
- [57] M. Ghiasi, and A. Malekzadeh, Synthesis of CaCO₃ Nanoparticles via Citrate Method and Sequential Preparation of CaO and Ca(OH)₂ Nanoparticles. *Crystal Research and Technology*. 4: 471–478 (2012).
- [58] C. V. Nnamani, O. C. Ani, and G. Belunwu, Larvicidal Effects of Ethanol Extracts of Leaves and

- Fruits of *Physalis angulata* L. on The Larvae of Anopheles Mosquitoes from ebonyi State, Nigeria. *Animal Research International*. 6: 1059-1062 (2009).
- [59] X. Wang, M. Wang, H. Song, & B. Ding, A simple sol–gel technique for preparing lanthanum oxide nanopowders. *Materials Letters*. 60, 17-18: 2261-2265 (2006).
- [60] M. Ghiasi, and A. Malekzadeh, Synthesis of CaCO₃ Nanoparticles via Citrate Method and Sequential Preparation of CaO and Ca(OH)₂ Nanoparticles. *Crystal Research and Technology*. 4: 471–478 (2012).
- [61] H. Doweidar, & Saddeek, Y. B. Effect of La₂O₃ on the structure of lead borate glasses. *Journal of non-crystalline solids*. 356, 28-30: 1452-1457 (2010).
- [62] M. Veerasingam, B. Murugesan, & S. Mahalingam, Ionic liquid mediated morphologically improved lanthanum oxide nanoparticles by *Andrographis paniculata* leaves extract and its biomedical applications. *Journal of Rare Earths*. 38, 3: 281-291 (2020).
-

(2021) ; www.mocedes.org/ajcer